Proceedings of the 2001 Particle Accelerator Conference, Chicago

DAMPING RINGS FOR CLIC

J.M. Jowett, T. Risselada, F. Zimmermann, CERN, Geneva, Switzerland
H. Owen, CLRC Daresbury Laboratory, United Kingdom

Abstract

The Compact Linear Collider (CLIC) is designed to operate at 3 TeV centre-of-mass energy with a total luminosity of 10^{35} cm^{-2}s^{-1}. The overall system design leads to extremely demanding requirements on the bunch trains injected into the main linac at a frequency of 100 Hz. In particular, the emittances of the intense bunches have to be about an order of magnitude smaller than presently achieved. We describe our approach to finding a damping ring design capable of meeting these requirements. Besides lattice design, emittance and damping rate considerations, a number of scattering and instability effects have to be incorporated into the optimisation of parameters. Among these, intra-beam scattering and the electron cloud effect are two of the most significant.

1 INTRODUCTION

Table 1 summarises the principal parameters required of the main damping rings by the CLIC design [1] for a linear collider operating at 3 TeV centre-of-mass energy. As shown in Figure 1, the requirements on normalised emittance are significantly smaller than in other linear collider designs. The now well-established principles of damping ring lattice design [2,3,4] lead to variants of a TME arc lattice augmented with damping wigglers in straight sections. However the resulting designs may not yield the desired performance because a variety of intensity-dependent effects—not usually taken account of in the initial design procedure—come into play.

Since a final choice has not been made for CLIC, and space is limited here, we illustrate two physical limitations on some typical lattices , indicating only their major features. Fuller details will appear elsewhere.

Quantity	Symbol	Value
Bunch population	N_b	4.1×10^{9}
No. of bunches/train	k_{bt}	154
Repetition frequency	f_r	100 Hz
Horizontal emittance	$\gamma\varepsilon_x$	4.5×10^{-7} m
Vertical emittance	$\gamma\varepsilon_y$	3×10^{-9} m
Bunch spacing	l_b	0.2 m
Min. kicker rise time	25	ns

Table 1: Beam parameters required for 3 TeV CLIC

2 INTRA-BEAM SCATTERING (IBS)

Damping rings are usually designed so that the required output emittance is reached within the time that a given bunch train spends in the ring, usually 4–5 damping times. IBS is sometimes taken into account by an iterative search for self-consistent final equilibrium emittances [7] (a fixed point of (1) below). Here we calculate the evolution of the emittances from injection into the damping ring to subsequent extraction and show that this equilibrium does not exist. (Our convention on the longitudinal emittance is $\varepsilon_t \approx \sigma_\delta \sigma_z$; σ_δ where σ_z are the RMS fractional energy spread and bunch length.)

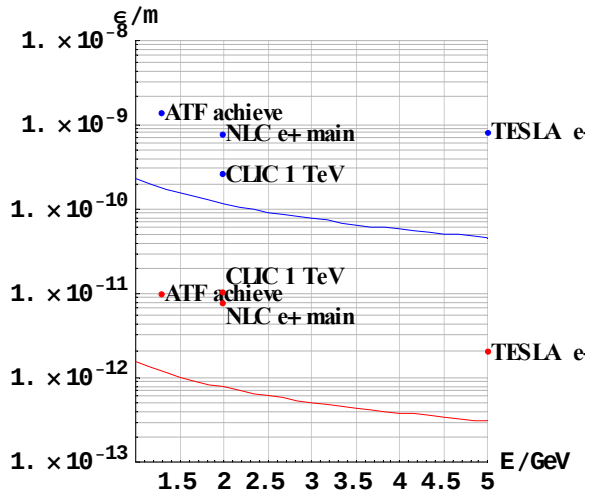

Figure 1: Geometric emittances vs. energy at the output of the main damping rings in various linear collider designs [3,4,5]. Values attained at the KEK ATF [6] are also shown. The 3 TeV CLIC requirements are plotted as blue (horizontal) and red (vertical) curves.

Assuming that rapid phase mixing has already taken place and taking into account the effects of radiation damping, quantum excitation and IBS, the emittances $\varepsilon_x, \varepsilon_y, \varepsilon_t$, of the three normal modes of single-particle motion evolve according to a set of three ordinary differential equations

$$\dot{\varepsilon}_\mu = -\frac{2}{\tau_\mu}\left(\varepsilon_\mu - \varepsilon_{\mu 0}\right) + \frac{2\varepsilon_\mu}{T_\mu\left(\varepsilon_x, \varepsilon_y, \varepsilon_t\right)}, \quad \mu \in \{x, y, t\} \qquad (1)$$

where τ_x, τ_y, τ_t are the radiation damping times and $\varepsilon_{x0}, \varepsilon_{y0}, \varepsilon_{t0}$ are the (geometric, *not* the "normalised") equilibrium emittances as determined by radiation damping and quantum excitation in the absence of IBS. The three equations are coupled through the IBS growth times $T_\mu\left(\varepsilon_x, \varepsilon_y, \varepsilon_t\right)$ which are non-linear functions [7] of the emittances and other beam parameters including the beam energy, E, and bunch population, N_b. In the present

calculation, we use the MAD [10] implementation of the Bjorken-Mtingwa theory [8], to sum local values of $T_\mu(\varepsilon_x, \varepsilon_y, \varepsilon_t)$ over all elements of our lattices. We pause to acknowledge that the MAD implementation of this theory has some limitations deriving from the common bias towards flat, uncoupled machines. However our damping rings closely approximate this archetype.

The numerical integration of the system (1) is carried out by Mathematica's **NDSolve** function [9] using dynamic programming to minimise the solicitation of MAD via the Madtomma [11] interface.

One of our first damping ring lattices ("**drv16**") at 1.98 GeV had circumference $C = 538$ m, including, besides the usual TME arcs, some 60 m of insertions containing 10.8 m of wigglers with a peak field of 1.8 T; neglecting IBS, this machine achieves the required ε_x. Another ring ("**drscale10**"),designed for 4.63 GeV, had similar straight sections but many more arc cells, giving a circumference of $C = 2419$ m; neglecting IBS, this machine betters the required ε_x by a factor 2.

The evolutions of the emittances for these two rings are shown in Figure 2. In **drv16**, ε_x and ε_y stay an order of magnitude above the required value while in **drscale10** they get within a factor ≈3. In both cases, ε_x begins to grow again as ε_y damps below a certain value. IBS is significant only for $\varepsilon_x, \varepsilon_y$ and then only when the injected emittances have damped sufficiently. This suggests that changes of the damping partition numbers at the expense of the longitudinal damping could be beneficial by slowing the damping of ε_t. Moreover, these calculations are arguably pessimistic for they do not include collective effects such as potential well or turbulent bunch lengthening that may sustain a larger ε_t for longer.

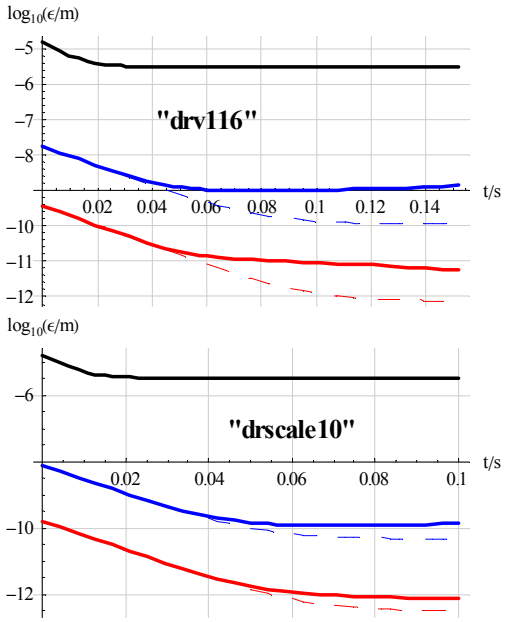

Figure 2: Evolution of ε_x (blue), ε_y (red) and ε_t (black) from injection to extraction (5 damping times). Dashed lines correspond to the absence of IBS.

3 ELECTRON CLOUD

We consider a set of typical parameters listed in Tables 1 and 2, assuming that both wiggler and arcs are equipped with an antechamber, which absorbs 95% of the photons. Only the remaining 5% contribute to the electron cloud generation via photoemission, with a supposed photoelectron yield of 5% per absorbed photon. We further assume that 10% of the photons escaping the antechamber are reflected towards the top and bottom of the beam pipe, whereas the other 90% remain confined within a narrow outward cone. A photoelectron that impinges on the wall may be lost, reflected or produce true secondary electrons. The maximum secondary emission yield for perpendicular incidence will vary as a function of electron bombardment. We consider values of δ_{max} between 1.7 and 1.1.

The dominant region of synchrotron radiation will be the long wiggler sections. Typical wiggler parameters are also given in the Table 2. In addition, there is of course synchrotron radiation in the arcs.

Quantity	Symbol	Value
Beam energy	E	3.5 GeV
RMS bunch length	σ_z	5 mm
RMS horiz. beam size	σ_x	18 μm
RMS vertical beam size	σ_y	1.5 μm
Average β-function	β_y	5 m
Wiggler period	λ_w	0.2 m
Peak field in wigglers	B_w	1 T
Wiggler deflection	θ_w	4.1 mrad
Arc dipole field	B_{arc}	0.015 T
Chamber radius	$h_{x,y}$	5 mm
Primary electron rate in wigglers	$d\lambda_e / ds$	0.075/ e^+/m
Primary e^- rate in arc	$d\lambda_e / ds$	0.0025/ e^+/m
Photon reflectivity	R	10%
Max. secondary emission yield	δ_{max}	1.1–1.7
Energy at δ_{max}	ε_{max}	300 eV
Max. probability of elastic reflection	$\delta_{el,E}$	0.56
Width of elastic reflection	σ_{el}	52 eV

Table 2: Parameters for electron cloud simulation

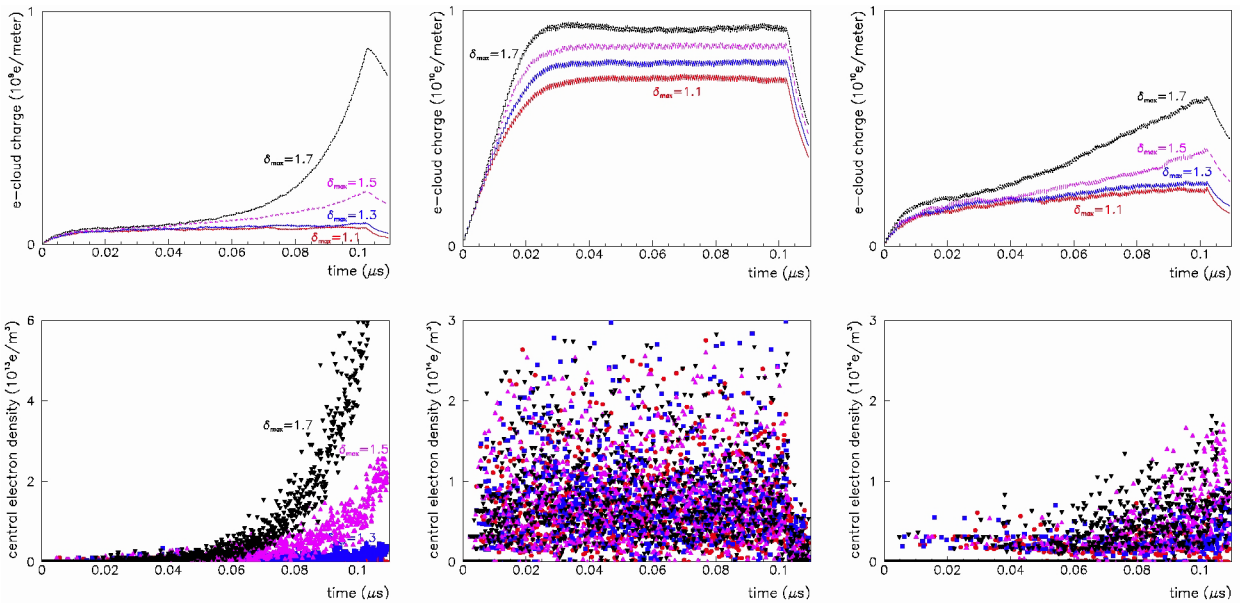

Figure 3: Evolution of electron cloud density (top row) and central cloud density (bottom row) as a function of time during the passage of the 154 bunch train through an arc chamber, a field free region adjacent to a wiggler and a periodic wiggler magnet. Results are shown for four different values of δ_{max} are shown (colours) and elastic electron scattering is included.

We simulate the electron cloud build-up for (1) a field-free region, (2) a bending field, (3) a periodic wiggler field, in all three cases considering a beam pipe illuminated by the wiggler radiation, and (4) for an arc dipole section, where the number of photoelectrons is reduced.

Simulations results are shown in Figure 3. The line density along the bunch train saturates at values of order $10^{10}\,\mathrm{m}^{-1}$. We note that the electron density is higher in the wigglers because of the larger number of primary photoelectrons. The difference between the periodic wiggler magnet and a uniform dipole field (also simulated but not shown) is small, assuming the same primary electron production rate. The central density near the beam attains values up to a few $10^{14}\,\mathrm{m}^{-3}$, a hundred times higher than the simulated and measured densities for the SPS or the two B factories, indicating that the electron cloud can pose a severe problem for damping rings.

The threshold density for the single-bunch TMCI instability driven by the cloud can be estimated as [12]

$$\rho_{e,\mathrm{th}}^{\mathrm{TMC}} \approx \frac{2\gamma Q_s}{\pi C r_e \beta_y} \qquad (2)$$

With $C \approx 2$ km, $\beta_y \approx 5$ m and $Q_s \approx 0.02$, we obtain $\rho_{e,\mathrm{th}}^{\mathrm{TMC}} \approx 3\times10^{12}\,\mathrm{m}$, 10–100 smaller than in Figure 3.

The coherent tune shift due to the cloud [13,14] is

$$\Delta Q_{x,y} \approx \frac{\beta_{x,y} C r_e \rho_e}{2\gamma} \qquad (3)$$

which, with the same parameters and $\rho_e \approx 10^{14}\,\mathrm{m}^{-3}$, evaluates to $\Delta Q_{x,y} \approx 0.2$. The incoherent tune spread can be several times larger still [13,14].

4 CONCLUSIONS

Damping rings for high-energy linear colliders like CLIC can suffer from severe electron cloud effects. Intra-beam scattering is also a major problem but can be taken account of in the design of the rings.

5 REFERENCES

[1] CLIC Study Team, "A 3 TeV e^+e^- Linear Collider based on CLIC Technology", CERN 2000-005 (2000).
[2] J.-P. Potier, L. Rivkin, PAC97, Vancouver, 1997.
[3] J.-P. Potier, T. Risselada, EPAC2000, Vienna, 2000.
[4] P. Emma, T. Raubenheimer, Phys. Rev. Special Topics Accelerators and Beams **4**, 021001 (2001).
[5] TESLA Technical Design Report, DESY 2001.
[6] K. Kubo, HEACC'01, Tsukuba 2001.
[7]A. Piwinski in A.W. Chao, M. Tigner (Eds.), *Handbook of Accelerator Physics and Engineering*, World Scientific, Singapore 1999.
[8] J.D. Bjorken, S.K. Mtingwa, Particle Accelerators **13** (1983) 115.
[9] S. Wolfram, *The Mathematica Book*, 4th ed., (Wolfram Media/Cambridge Unv. Press) 1999.
[10] http://wwwslap.cern.ch/mad/
[11] http://cern.ch/jowett/Madtomma/
[12] K. Ohmi and F. Zimmermann, Phys. Rev. Letters 85, p. 3821 (2000).
[13] M. Furman and A. Zholents, PAC99, (1999).
[14] F. Zimmermann, in CERN-SL-2001-003-DI (2001).